Asian Research Journal of Mathematics
2(4): 1-19, 2017; Article no.ARJOM.31306
ISSN: 2456-477X

SCIENCEDOMAIN *international*
www.sciencedomain.org

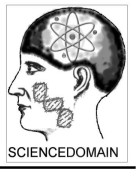

Steady Oscillatory Flow in a Bifurcating Green Plant

W. I. A. Okuyade[1*] and T. M. Abbey[2]

[1]Department of Mathematics and Statistics, University of Port Harcourt, Port Harcourt, Nigeria.
[2]Applied Mathematics and Theoretical Physics Group, Department of Physics, University of Port Harcourt, Port Harcourt, Nigeria.

Authors' contributions

This work was carried out in collaboration between both authors. They read and approved the final manuscript.

Article Information

DOI: 10.9734/ARJOM/2017/31306
Editor(s):
(1) Hari Mohan Srivastava, Department of Mathematics and Statistics, University of Victoria, Canada.
Reviewers:
(1) Saima Fazal, South China University of Technology, China.
(2) Bhim Sen Kala, K L University, Guntur, Andhra Pradesh, India.
(3) P. Sulochana, Intell Engineering College, Anantapuramu, Andhra Pradesh, India.
Complete Peer review History: http://www.sciencedomain.org/review-history/17836

Original Research Article

Received: 30th December 2016
Accepted: 4th February 2017
Published: 15th February 2017

Abstract

Steady oscillatory flow in a bifurcating green plant is investigated. The channel is assumed axisymmetrical and porous; the fluid is Newtonian, incompressible, electrically conducting and chemically reactive but of the order one homogeneous type. The models are developed using the Boussinesq's approximations. The nonlinear and coupled equations governing the flow are non-dimensionalized and solved analytically using the similarity transformation and perturbation series solutions. Expressions for the concentration, temperature and velocity are obtained and presented in tabular form. The results show that the increase in the chemical reaction rate, Hartmann number (for $0.1 \leq M^2 \leq 1.0$), Heat generation parameter, Grashof number (for $0.1 \leq Gr \leq 1.0$), Peclet number and Reynolds number increase the concentration and velocity, and specifically, the increase in the bifurcation angle decreases the concentration but increases the velocity. Furthermore, it is seen that for Hartmann number $M^2 \geq 5.0$ the velocity drops. This model has relevance to agriculture. In fact, the increase in the flow variables enhances the growth and yield of plant (crops).

Keywords: Bifurcation; green plants; MHD; oscillatory flow; porous channel.

**Corresponding author: E-mail: wilsonia6011@gmail.com;*

1 Introduction

A number of studies have been carried out on the flow of soil mineral salt water and manufactured/synthesized materials in the green plants. Some studied the flow through the leaves, some the roots, and others the tree trunk. On the flow through the tree trunk, [1] studied the flow dynamics of soil mineral salt water upward and that of manufactured/synthesized materials in the leaves downward a tree trunk whose aspect ratio (the ratio of the length to the diameter) is far less than one. That is, $\Re = \frac{d}{l} << 1$. According to him, such flow is laminar, Poiseuille and fully developed. Such model tends to be applicable to flow in trees like iroko, palm tree, paw-paw, plantains and the likes. The model has some limitations. It did not consider the case where the aspect ratio is approximately greater than or equal to one (i.e. $\Re \geq 1$), a situation in which bifurcation angle and Reynolds number play effective roles, as may be seen in plants that furcated early in their growth stage such as pears, mangoes, guava, and so on; the effects of the nature of the soil on which the plant grows, and positive environmental temperature changes on the flow.

More so, his solutions show the existence of imaginary parts. He did not emphasize their contributions, which are exhibited in the form of oscillatory motion. Therefore, in this paper, we are motivated to investigate the oscillatory flow characteristics of the soil mineral salt water through the trunk of a bifurcating green plant, taking cognizance of the nature of the soil on which the plant grow, and positive environmental temperature changes on the flow.

Reports exist in literature on some related flow behaviours in both bifurcating and non-bifurcating systems. For example, [2-4] in their various ways studied the flow in bifurcating channels and noticed that the increase in bifurcation angle and Reynolds number increase the transport velocity; [5] examined the steady fully developed laminar flow through a pipe by experimental and finite difference numerical scheme, and observed among others, that the axial velocity asymptotically approaches its limit as the Hartmann number becomes large; [6] studied the MHD free convection flow through a vertical porous channel using the finite difference numerical approach, and noticed that the velocity decreases with the increase in the magnetic and porosity parameters; [7] examined the the oscillatory flow of a viscous incompressible Newtonian fluid in an infinite vertical parallel plate channel filled wih porous media using the method of double perturbation, and obtained the approximate solutions to the coupled nonlinear partial differential equations governing the flow; [8] studied two-dimensional flow of Jeffery fluid with small suction in a rectangular channel , wherein they investigated the viscoelastic behaviour of non-Newtonian fluids subject to time harmonic oscillation using the perturbation method of Wentz- Krammer-Brillouin (WKB) and variation of parameter , and found that the amplitude and penetration depth decrease with the increase in the suction parameter and compression of the wave; the decrease in the penetration depth are higher in Jeffery fluid than in viscous fluids with increasing suction on the wall; [9] considered the fully developed MHD mixed convective flow in a vertical channel filled with nano-fluids using the closed form solutions, and noticed that magnetic field enhances the nano-fluid velocity. Even so, [10] studied the magneto-hydrodynamic free convective and oscillatory flow through a vertical porous channel and found amidst others, that the flow velocity increases with the increase in the Grashof number but decreases due to increase in the porosity parameter or magnetic parameter; [11] investigated the MHD convective force flow in bifurcating porous fine capillaries, and found that magnetic field reduces the flow velocity, whereas the convective force increases it. More so, [12] considered analytically a span-wise fluctuating magneto-hydrodynamic (MHD) convective flow of a viscous, incompressible and electrically conducting fluid through an infinite vertical porous channel, with the walls subjected to span-wise cosinusoidally varying species concentration and temperature. They observed among others, that the velocity increases with the increase in the buoyancy forces due to concentration and thermal diffusions, and permeability but decreases with the increase in the magnetic field, Prandtl number, heat generation/absorption parameter. [13] elaborately investigated analytically the MHD free convective three-dimensional flow of an incompressible viscous fluid in a vertical parallel plates channel filled with a porous medium, and observed amidst others, that the velocity component for the primary flow enhances with the increase in Reynolds number, Darcy parameter, hall parameter, Grashof

number, Peclet number and pressure gradient but reduces with the increase in the intensity in magnetic field and radiation parameter; [14] studied numerically the unsteady heat and mass transfer flow with a temperature dependent viscosity past an isothermal oscillating cylinder using the method of finite difference, and observed among others that the increase in the Schmidt number, Prandtl number, Hartmann number decrease the velocity; the increases in the chemical reaction rate and viscosity variation parameters decrease the concentration, the increase in the chemical reaction rate parameter decreases the skin friction; the increase in the viscosity variation parameter decreases the Nusselt number .

In this study, we investigate the effects of chemical reaction rate, heat exchange parameter, Hartmann, Grashof, Peclet, and Reynolds numbers, and bifurcation angles on the oscillatory flow of soil mineral salt water through the trunk of a bifurcating green plant whose aspect ratio is approximately equal to or greater than one.

The paper is organized in the following manner: section 2 is the methodology; section 3 is the results and discussion, and section 4 holds the conclusions.

2 Methodology

Natural systems such as plants are cylindrical and porous. The soil mineral salt water is, by the nature of its chemical content a magneto-fluid. The fluids in plants are not pumped by any physical means. Therefore, through the effects of external/environmental temperature and concentration differentials, their flow is naturally convective. The Reynolds number of the flow is much less than one (i.e. Re<1) such that the flow is creepy (see [1]). Let (r', θ', x') and (u', v', w') be the polar orthogonal coordinates and velocity components, respectively. We assumed the velocity is axisymmetrical about the θ' axis such that variations about θ' is zero and as such the coordinates and velocity components are reduced to (r', x') and (u', w'). Then, the mathematical models describing the flow of the fluid in a bifurcating green plant as shown in Fig 1, considering Boussinesq approximations are

$$\frac{1}{r}\frac{\partial}{\partial r}\left(r'u'\right)+\frac{\partial w'}{\partial r'}=0 \tag{1}$$

$$0=-\frac{\partial p'}{\partial r'}+\mu\left(\frac{\partial^2 u'}{\partial r'^2}+\frac{1}{r'}\frac{\partial u'}{\partial r'}+\frac{u'}{r'^2}+\frac{\partial^2 u'}{\partial x'^2}\right) \tag{2}$$

$$0=-\frac{\partial p'}{\partial x'}+\mu\left(\frac{\partial^2 w'}{\partial r'^2}+\frac{1}{r'}\frac{\partial w'}{\partial r'}+\frac{\partial^2 w'}{\partial x'^2}\right)+\rho g\beta_t\left(T'-T_\infty\right)+\rho g\beta_C\left(C'-C_\infty\right)-\left(\frac{\mu}{\kappa}+\frac{\sigma_e B_o^2}{\rho^2\mu_m}\right)w' \tag{3}$$

$$u'\frac{\partial T'}{\partial r'}+w'\frac{\partial T'}{\partial x'}=-\frac{k}{\rho C_p}\left(\frac{\partial^2 T'}{\partial r'^2}+\frac{1}{r'}\frac{\partial T'}{\partial r'}+\frac{\partial^2 T'}{\partial x'^2}+\frac{Q\left(T'-T_\infty\right)}{\rho C_p}\right) \tag{4}$$

$$u'\frac{\partial C'}{\partial r'}+w'\frac{\partial C'}{\partial x'}=-D\left(\frac{\partial^2 C'}{\partial r'^2}+\frac{1}{r'}\frac{\partial C'}{\partial r'}+\frac{\partial^2 C'}{\partial x'^2}+k_r^2\left(C'-C_\infty\right)\right) \tag{5}$$

where ρ the fluid density, p' the pressure, μ the viscosity, μ_m the magnetic permeability of the fluid, **g** the gravitational field vector acting in the reverse direction of the flow, T' and C' are, respectively, the fluid temperature and concentration (quantity of material being transported), while T_w and C_w are the constant wall temperature and concentration at which the channel is maintained, whereas T_∞ and C_∞ are, respectively, the temperature and concentration at equilibrium, κ is the permeability parameter of the porous medium, B_o^2 is the applied uniform magnetic field strength due the nature of the soil and the earth field, σ_e is the electrical conductivity of the fluid, k_o the thermal conductivity, C_p the specific heat capacity at constant pressure, Q is the heat generation/absorption coefficient, D the diffusion coefficient, k_r^2 is the rate of chemical reaction of the soil mineral salt solution.

The analysis considers a homogeneous first order chemical reaction (a reaction which is proportional to the concentration) with constant rate k_r^2 between the diffusing species and the fluid; the porous medium is non-homogeneous, therefore, its permeability is anisotropic; the fluid is assumed to have constant properties except that its density varies with the temperature and concentration; the viscosity of the fluid is a function of the temperature and magnetic field; the applied magnetic field and magnetic Reynolds number are assumed to be very small so that the induced magnetic field and hall effects are negligible.

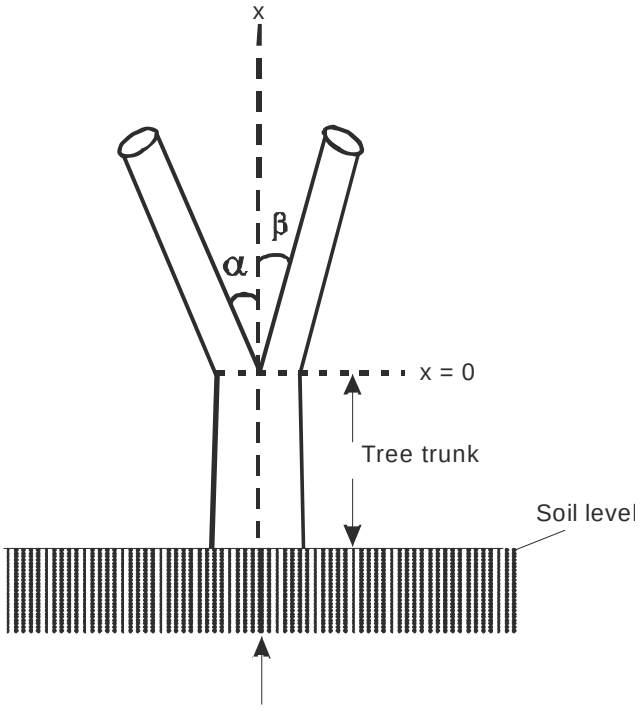

Fig. 1. The physical representation of the model

The general analysis of the physical geometry of the problem presented in Fig. 1 shows that the boundary conditions can be split into two distinct parts, namely, the upstream, $x' < 0$ and the downstream, $x' > 0$. The flow in the mother is laminar and Poiseuille with the characteristic parabolic profile. The local stream-wise direction in the mother tube is x' while in the daughter tube, it is off the x' - axis. The problem of the wall curvature on the geometrical transition between the mother and the daughter tubes exists. To fix up the

role of curvature, a very simple transition wherein the radius of the daughter is assumed equal to that of the mother and the variation of the bifurcation angle is straight-forwardly used (see [4]).

The boundary conditions are as follows:

In the upstream/mother channel

$$u^{'} = 1, w^{'} = 1, T^{'} = T_{\infty}, C^{'} = C_{\infty} \quad \text{at } r^{'} = 0 \tag{6}$$

$$u^{'} = 0, w^{'} = 0, T^{'} = T_{w}, C^{'} = C_{w} \quad \text{at } r^{'} = 1 \tag{7}$$

and in the downstream(daughter channel)

$$u^{'} = 0, w^{'} = 0, T^{'} = 0, C^{'} = 0 \quad \text{at } r^{'} = 0 \tag{8}$$

$$u^{'} = 0, w^{'} = 0, T^{'} = \gamma_1 T_w, C^{'} = \gamma_2 C_w, \gamma_{1,} = \gamma_2 < 1 \quad \text{at } r^{'} = \alpha x^{'} \tag{9}$$

Introducing the following non-dimensionalized variables into equations (1) - (9),

$$u = \frac{u'}{l}, \quad r = \frac{r'}{R_o}, x = \frac{\Re x'}{l}, w = \frac{w' R_o}{\upsilon}, \Theta = \frac{T^{'} - T_{\infty}}{T_w - T_{\infty}}, \Phi = \frac{C^{'} - C_{\infty}}{C_w - C_{\infty}},$$
$$p = \frac{(p' - p_{\infty}) r_o^3}{\rho l \upsilon}, \mathrm{Re} = \upsilon l, M^2 = \frac{\sigma_e B_o^2}{\rho \mu \mu_m}, N^2 = \frac{Q}{k_o}, \chi^2 = \frac{R_o}{\kappa}, \delta_1^2 = \frac{k_r^2}{D},$$
$$Sc = \frac{\upsilon}{D}, \mathrm{Pr} = \frac{\mu Cp}{k_o}, Gr = \frac{g\beta_1 (T_w - T_{\infty})}{\upsilon^2}, Gc = \frac{g\beta_2 (C_w - C_{\infty})}{\upsilon^2}$$

where Pe_m = Re Sc , Pe_h = Re Pr , $M_1^2 = \chi^2 + M^2$, $\beta 1$ and β_2 are the volumetric expansion coefficient for temperature and concentration respectively, Θ and Φ are the non-dimensionalized temperature and concentration, respectively, $\Re$ is the aspect ratio, υ is the kinematic viscosity, R_o is the characteristic radius of the tree trunk, M^2 is the soil parameter, Re is the Reynolds number, N^2 is the heat exchange parameter, χ^2 is the porosity parameter, δ_1^2 is the chemical reaction parameter, Sc the Schmidt number, Pr the Prandtl number, (Gr, Gc) are the Grashof number due to temperature and concentration differences, while (Pe_h , Pe_m) are the Peclet number due to heat and mass transfers, we have

$$\frac{1}{r}\frac{\partial (ru)}{\partial r} + \frac{\Re \partial w}{\partial x} = 0 \tag{10}$$

$$\frac{\partial^2 u}{\partial r^2} + \frac{1}{r}\frac{\partial u}{\partial r} - \frac{u}{r^2} = \frac{\partial p}{\partial r} \tag{11}$$

$$\frac{\partial w}{\partial r'} + \frac{1}{r}\frac{\partial w}{\partial r} - (M^2 + \chi^2) w = \Re \frac{\partial p}{\partial x} - Gr\Theta - Gc\Phi \tag{12}$$

$$\frac{\partial^2\Theta}{\partial r^2}+\frac{1}{r}\frac{\partial\Theta}{\partial r}+N^2\Theta=Pe_h(u\frac{\partial\Theta}{\partial r}+\Re w\frac{\partial\Theta}{\partial x}) \tag{13}$$

$$\frac{\partial^2\Phi}{\partial r^2}+\frac{1}{r}\frac{\partial\Phi}{\partial r}+\delta_1^2\Phi=Pe_m(u\frac{\partial\Phi}{\partial r}+\Re w\frac{\partial\Phi}{\partial x}) \tag{14}$$

with the boundary conditions:

for the upstream (mother channel):

$$\text{u= 0, w = 0 and } \Theta=\Theta_w,\ \Phi=\Phi_w \quad \text{at r = 1} \tag{15}$$

and for the downstream/daughter channel:

$$\text{u = 0, w = 0 and } \Theta=\gamma_1\Theta_w,\Phi=\gamma_2\Phi_w \quad \text{at } r=\Re\alpha x \tag{16}$$

Equations (10)-(16) are nonlinear and coupled. Therefore, we seek for solutions of the form

$$f(r,x)=f_o(r,x))+\xi f_1(r,x)+\xi^2 f_2(r,x)+... \tag{17}$$

where $\xi=\mathrm{Re}<1$ the perturbing parameter, is extremely small (about Re=0.1). The choice of this parameter is based on the fact that, in the mother channel, the flow is laminar and Poiseuille. Nevertheless, as the fluid flows towards the point of bifurcation, it experiences some forms of disturbances due to a change in the geometrical configuration and its inertial force rises, with subsequent increase in the Reynolds number and momentum. Assuming a flow field of the form such that

$$\frac{\partial u}{\partial r}=\frac{\partial p}{\partial r}=0,\ f_0(r,x)=f_{00}(r)-\gamma x \text{ and } f_1(r,x)=f_{10}(r)-\gamma x,\ p=\aleph x-\frac{\aleph x^2}{\Re}$$

where f_0 and f_1 represents the velocity, temperature and concentration in the mother (or upstream) and daughter (or downstream) sections, respectively; $\aleph x$ is the pressure in the mother region; $\frac{\aleph x^2}{\Re}$ is the pressure in the daughter region (see [1]), then the equations governing the flow in these streams are as follows:

$$\frac{\partial^2 w_{00}}{\partial r^2}+\frac{1}{r}\frac{\partial w_{00}}{\partial r}-M_1^2 w_{00}=\frac{\Re\partial p_{00}}{\partial x}-Gr\Theta_{00}-Gc\Phi_{00} \tag{18}$$

$$\frac{\partial^2\Theta_{00}}{\partial r^2}+\frac{1}{r}\frac{\partial\Theta_{00}}{\partial r}+N^2\Theta_{00}=-\gamma\Re Pe_h w_o \tag{19}$$

$$\frac{\partial^2\Phi_{00}}{\partial r^2}+\frac{1}{r}\frac{\partial\Phi_{00}}{\partial r}+\delta_1^2\Phi_{00}=-\gamma\Re Pe_m w_o \tag{20}$$

with the boundary conditions

$$w_{00} = 1,\ \Theta_{00} = 1,\ \Phi_{00} = 1 \text{ at } \quad r = 0 \tag{21}$$

$$w_{00} = 0,\ \Theta_{00} = \Theta_w,\ \Phi_{00} = \Phi_w \quad \text{at } \ r = 1 \tag{22}$$

for the upstream and

$$\frac{\partial^2 w_{10}}{\partial r^2} + \frac{1}{r}\frac{\partial w_{10}}{\partial r} - M_1^2 w_{10} = \Re \frac{\partial p_{10}}{\partial x} - Gr\Theta_{10} - Gc\Phi_{10} \tag{23}$$

$$\frac{\partial^2 \Theta_{10}}{\partial r^2} + \frac{1}{r}\frac{\partial \Theta_{10}}{\partial r} + N^2\Theta_{10} = -\Re Pe_h\left(w_{00}\frac{\partial \Theta_{10}}{\partial x} + w_{10}\frac{\partial \Theta_{00}}{\partial x}\right) \tag{24}$$

$$\frac{\partial^2 \Phi_{10}}{\partial r^2} + \frac{1}{r}\frac{\partial \Phi_{10}}{\partial r} + \delta_1^2\Phi_{10} = -\Re Pe_m\left(w_{00}\frac{\partial \Phi_{10}}{\partial x} + w_{10}\frac{\partial \Phi_{00}}{\partial x}\right) \tag{25}$$

with the boundary conditions

for the upstream/mother channel:

$$w_{10} = 0,\ \Theta_{10} = 0\ ,\ \Phi_{10} = 0 \text{ at } \quad r = 0 \tag{26}$$

and for the downstream/daughter channel:

$$w_{10} = 0,\ \Theta_{10} = \gamma_1\Theta_w,\ \Phi_{10} = \gamma_2\Phi_w,\ \gamma_1 < 1,\ \gamma_2 < 1 \quad \text{at} \quad r = \Re\alpha x \tag{27}$$

where $\aleph_1 = -2\gamma$

Now, for the upstream, we shall eliminate w_o from equations (19) and (20) by taking the

$$\left(\frac{\partial^2}{\partial r^2} + \frac{1}{r}\frac{\partial}{\partial r} - M_1^2\right)$$

of both equations to get

$$\left[\left(D_r - M_1^2\right)\left(D_r + N^2\right) - \gamma R\varepsilon\right]\Theta_{oo} = \gamma R\varepsilon\Phi_{oo} - \gamma\Re\varepsilon Pe_h\aleph \tag{28}$$

and

$$-\gamma\Re\varepsilon Pe_h\aleph + \gamma R\varepsilon\Theta_{oo} = \left[\left(D_r - M_1^2\right)\left(D_r + \delta_1^2\right) - \gamma R\varepsilon\right]\Phi_{oo} \tag{29}$$

where

$$D_r = \left(\frac{\partial^2}{\partial r^2} + \frac{1}{r}\frac{\partial}{\partial r} \right) \text{and } \varepsilon = Pe_h Gr = Pe_m Gc, Gr = Gc$$

By further rationalization, we shall eliminate Θ_{oo} from equations (28) and (29) by multiplying through equation (28) by $\gamma R\varepsilon$ and taking

$$\left[\left(D_r - M_1^2 \right) \left(D_r + N^2 \right) - \gamma R\varepsilon \right]$$

of equation (29) so that on adding the first result to the second, and rearranging, we have

$$\left[\left(D_r - M_1^2 \right)\left(D_r + N^2 \right) - \gamma R\varepsilon \right]\left[\left(D_r - M_1^2 \right)\left(D_r + \delta_1^2 \right) - \gamma R\varepsilon \right]\Phi_{oo} = -\gamma R\varepsilon Pe_h \aleph \tag{30}$$

and which on expanding gives

$$\begin{aligned} &\left[D_r^4 + \left(2N^2 + \delta_1^2 - M_1^2 \right) D_r^3 + \left(-M_1^2 + 2N^2 M_1^2 + 2M_1^2 - N^2\delta_1^2 - M_1^4 - 2\gamma R\varepsilon \right) D_r^2 + \right. \\ &\left. \left(-M_1^4\delta_1^2 - \gamma\Re\varepsilon\left(2N^2 - M^2 - \delta_1^2 + M_1^2 N^4 \right) \right) D_r + \left(-M_1^2\delta_1^2\gamma\Re\varepsilon + \gamma^2\Re^2\varepsilon^2 \right) \right]\Phi_{oo} \\ &\qquad = -\gamma R\varepsilon Pe_h \aleph \end{aligned} \tag{31}$$

This is a fourth order characteristic equation. We shall split it into two tractable parts: The even and odd powers terms. Thus:

$$\begin{aligned} &\left[D_r^4 + \left(-M_1^2 + 2N^2 M_1^2 + 2M_1^2 - N^2\delta_1^2 - M_1^4 - 2\gamma R\varepsilon \right) D_r^2 + \right. \\ &\left. \left(-M_1^2\delta_1^2\gamma\Re\varepsilon + \gamma^2\Re^2\varepsilon^2 \right) \right]\Phi_{oo} \quad = -\gamma R\varepsilon Pe_h \aleph \end{aligned} \tag{32}$$

for the even power terms

$$D_r \left[\left(2N^2 + \delta_1^2 - M_1^2 \right) D_r^2 + \left(-M_1^4\delta_1^2 - \gamma\Re\varepsilon\left(2N^2 - M^2 - \delta_1^2 + M_1^2 N^4 \right) \right) \right]\Phi_{oo} = 0 \tag{33}$$

and for the odd powers terms.

Since our problem is of fourth order, we shall solve only equation (32) and use the results to approximate the solution of our problem. And, the solution is

$$\Phi_{oo}(r) = D_1 I_o\left(\lambda_8^{1/2} r \right) + \frac{I_o\left(\lambda_8^{1/2} r \right)}{2} \lambda_8^{1/2} C_1 \frac{r I_1\left(\lambda_6^{1/2} r \right)}{\lambda_6^{1/2}} \tag{34}$$

Furthermore, assuming $\Pr Gr = \Pr Gc$ and $\Phi_{oo} = \Theta_{oo}$, substituting Φ_{oo} and Θ_{oo} in equation (18) and solving, we have

$$w_{oo}(r) = V_1 I_o(M_1 r) - M_1 r I_o(M_1 r)\left[-\frac{\Re \aleph r}{2} + GrD_1 \frac{I_1(\lambda_8^{1/2} r)}{\lambda_6^{1/2}} + \right.$$
$$\left. -\frac{r^5}{20} - \frac{\lambda_6 r^7}{114} + M_1^2\left(\frac{r^4}{16} + \frac{\lambda_6 r^6}{192}\right)\right] + \left(-\frac{M_1 r}{2} + \frac{M_1^2 r^3}{4}\right)\left[\frac{\Re \aleph I_1(M_1 r)}{M_1} - 2GrD_1\left(\frac{I_1(\lambda_8^{1/2} r)}{\lambda_8^{1/2}} - \right.\right.$$
$$\left.\left. \frac{M_1^2 r^3}{6} - \frac{M_1^2 \lambda_8 r^5}{40}\right) + \frac{r^3}{6} + \frac{\lambda_6 r^5}{80} + M_1^2\left(\frac{r^4}{16} + \frac{\lambda_6 r^6}{192}\right)\right] \quad (35)$$

Similarly, eliminating Φ_{oo} from equations (28) and (29) by taking

$$\left[\left(D_r - M_1^2\right)\left(D_r + \delta_1^2\right) - \gamma R\varepsilon\right]$$

of equation (28) and multiplying through equation (29) by $\gamma R\varepsilon$ so that on adding the two results gives

$$\left[\left(D_r - M_1^2\right)\left(D_r + N^2\right) - \gamma R\varepsilon\right]\left[\left(D_r - M_1^2\right)\left(D_r + \delta_1^2\right) - \gamma R\varepsilon\right]\Theta_{oo} = -\gamma R\varepsilon Pe_h \aleph \quad (36)$$

A comparison of equation (30) with equation (36) shows that they are the same. Therefore, $\Phi_{oo} = \Theta_{oo}$, and so are their solutions.

For the downstream, we consider equations (23) - (25). We shall eliminate

w_{oo} and w_{10} from equations (24) and (25) by taking

$$\left(\frac{\partial^2}{\partial r^2} + \frac{1}{r}\frac{\partial}{\partial r} - M_1^2\right)$$

of both sides of the equations to get

$$\left[\left(D_r - M_1^2\right)\left(D_r + N^2\right)\right]\Theta_{10} = -\gamma R^2 Pe_h\left(\aleph + \aleph_1 x\right) + \gamma R\varepsilon\left(\Theta_{10} + \Phi_{10}\right) + \gamma R\varepsilon\left(\Theta_{oo} + \Phi_{oo}\right) \quad (37)$$

and

$$\left[\left(D_r - M_1^2\right)\left(D_r + \delta^2\right)\right]\Phi_{10} = -\gamma R^2 Pe_h\left(\aleph + \aleph_1 x\right) + \gamma R\varepsilon\left(\Theta_{10} + \Phi_{10}\right) + \gamma R\varepsilon\left(\Theta_{oo} + \Phi_{oo}\right) \quad (38)$$

By the already known solutions of Θ_{oo} and Φ_{oo} [see eq. (34)], equations (37) and (38) respectively, become

$$\left[\left(D_r - M_1^2\right)\left(D_r + N^2\right) - \gamma R\varepsilon\right]\Theta_{10} = \gamma R\varepsilon\Phi_{10} - \gamma R^2 Pe_m\left(\aleph + \aleph_1 x\right) + 2\gamma R\varepsilon D_1 I_o\left(\lambda_6^{1/2} r\right) \quad (39)$$

and

$$\left[\left(Dr - M_1^2\right)\left(Dr + \delta_1^2\right) - \gamma R\varepsilon\right]\Phi_{10} = \gamma R\varepsilon\Theta_{10} - \gamma R^2 Pe_m\left(\aleph + \aleph_1 x\right) + 2\gamma R\varepsilon D_1 I_o\left(\lambda_6^{1/2} r\right) \quad (40)$$

More so, eliminating Θ_{10} from equations (39) and (40) by multiplying through equation (39) by $\gamma\Re\varepsilon$ and taking

$$\left[\left(D_r - M_1^2\right)\left(D_r + N^2\right) - \gamma\Re\varepsilon\right]$$

of equation (40), respectively, and the subtracting the first result from the second, we have

$$\begin{aligned}&\left[\left(D_r - M_1^2\right)\left(D_r - N^2\right) - \gamma\Re\varepsilon\right]\left[\left(D_r - M_1^2\right)\left(D_r - \delta_1^2\right) - \gamma\Re\varepsilon\right]\Phi_{10} - \gamma^2\Re^2\varepsilon^2\Phi_{10} \\ &\quad = -\gamma^2\Re^3\varepsilon Pe_h\left(N + N_1 x\right) + 2D_1\gamma^2\Re^2\varepsilon^2 I_o\left(\lambda_6^{1/2} r\right)\end{aligned} \tag{41}$$

which on expanding gives

$$\begin{aligned}&\left\{\begin{array}{l} D_r^4 + \left[\left(\delta_1^2 - M_1^2\right)\left(N^2 - M_1^2\right)D_r^3\right] + \left[-M_1^2\delta_1^2 + \left(N^2 - M_1^2\right)\left(\delta_1^2 - M_1^2\right) - M_1^2 N^2\right]D_r^2 \\ \left[-M_1^2\delta_1^2\left(N^2 - M_1^2\right) - \gamma\Re\varepsilon\left(N^2 - M_1^2\right) - M_1^2 N^2\left(\delta_1^2 - M_1^2\right) - \gamma\Re\varepsilon\left(\delta_1^2 - M_1^2\right)\right]D_r + \\ \gamma\Re\varepsilon\left[M_1^2 N^2\delta_1^2 + M_1^2 N^2 + M_1^2\delta_1^2\right] \end{array}\right\}\Theta_{10} \\ &\quad = \gamma^2\Re^3\varepsilon Pe_h\left(N + N_1 x\right) + D_1\gamma^2\Re^2\varepsilon^2 I_o\left(\lambda_6^{1/2} r\right)\end{aligned} \tag{42}$$

Splitting this into the even and odd power terms, we get

$$\begin{aligned}&\left[D_r^4 + \left[-M_1^2\delta_1^2 + \left(N^2 - M_1^2\right)\left(\delta_1^2 - M_1^2\right) - M_1^2 N^2\right]D_r^2 + \gamma\Re\varepsilon\left[M_1^2 N^2\delta_1^2 + M_1^2 N^2 + M_1^2\delta_1^2\right]\right]\Theta_{10} \\ &\quad = \gamma^2\Re^3\varepsilon Pe_h\left(N + N_1 x\right) + D_1\gamma^2\Re^2\varepsilon^2 I_o\left(\lambda_6^{1/2} r\right)\end{aligned} \tag{43}$$

for the even power terms, and

$$\begin{aligned}D_r\left[\left[\left(\delta_1^2 - M_1^2\right)\left(N^2 - M_1^2\right)\right]D_r^2 + \left[-M_1^2\delta_1^2\left(N^2 - M_1^2\right) - \gamma\Re\varepsilon\left(N^2 - M_1^2\right)\right.\right. \\ \left.\left. - M_1^2 N^2\left(\delta_1^2 - M_1^2\right) - \gamma\Re\varepsilon\left(\delta_1^2 - M_1^2\right)\right]\right]\Theta_{10} = 0\end{aligned} \tag{44}$$

for the odd terms

We shall solve only equation (43), and use its solution to approximate that of our problem. And, the solution is

$$\Phi_{10} = K_1\frac{I_o\left(\lambda_{16}^{1/2} r\right)}{2} + I_o\left(\lambda_{16}^{1/2} r\right)\lambda_{16}^{1/2} G_1 r\frac{I_o\left(\lambda_{14}^{1/2} r\right)}{\lambda_{14}^{1/2}} \tag{45}$$

Moreover, assuming $\Phi_{10} = \Theta_{10}$, substituting Φ_{10} and Θ_{10} in equation (23) and solving, we have

$$w_1(r) = V_1 I_o(M_1 r) - I_o(M_1 r)\left\{-\frac{\Re \aleph_1 xr}{2} + Gc\left[\frac{K_1 I_1(\lambda_{16}^{1/2} r)}{\lambda_{16}^{1/2}} + \lambda_{16}^{1/2} G_1\left(\frac{rI_1(\lambda_{16}^{1/2} r)}{\lambda_{16}^{1/2}} + \frac{\lambda_{14} r^4}{64} + \frac{\lambda_{14}\lambda_{16} r^6}{384}\right)\right]\right.$$
$$+\frac{M_1^2}{4}\left[\frac{\Re \aleph_1 r^3}{3} - 2Gc\left[K_1\left(\frac{r^3}{3} + \frac{\lambda_{16} r^5}{20}\right) + \lambda_{16}^{1/2} G_1\left(\frac{rI_1(\lambda_{16}^{1/2} r)}{2\lambda_{16}^{1/2}}\right.\right.\right.$$
$$\left.\left.\left.\left. + \frac{\lambda_{14} r^4}{64} + \frac{\lambda_{14}\lambda_{16} r^6}{384}\right)\right]\right]\right\} + \left(-\frac{M_1 r}{3} + \frac{M_1^3 r^3}{4}\right)\left\{-\frac{\Re \aleph_1 xI_1(M_1 r)}{M_1}\right.$$
$$+ 2Gc\left[K_1\left(\frac{I_1(M_1 r)}{M_1} + \frac{\lambda_{16} r^4}{16} + \frac{M_1^2 \lambda_{16} r^5}{80}\right) + \lambda_{16}^{1/2} G_1\left(\frac{rI_1(M_1 r)}{2M_1} + \frac{\lambda_{14} r^4}{64} + \frac{\lambda_{14} M_1 r^6}{384}\right)\right.$$
$$\left.\left. + \frac{\lambda_{16} r^4}{32} + \frac{\lambda_{16} M_1^2 r^6}{192} + \frac{\lambda_{14}\lambda_{16} r^6}{384} + \frac{\lambda_{14}\lambda_{16} M_1^2 r^8}{2048}\right]\right\} \tag{46}$$

3 Results and Discussion

Using the Maple 18 computational software, we computed for constant realistic values of Pr =0.71, γ_1 = 0.6, γ_2 =0.6, γ =0.7, Φ_w = 2.0, Θ_w =2.0, $\Re = 0.8$ and varying values of δ_1^2 =0.1, 0.3, 0.5, 1.0, 5.0; M^2 = 0.1, 0.3, 0.5, 1.0, 5.0; N^2=0.1, 0.3, 0.5, 1.0, 5.0; Gr/Gc=0.1, 0.3, 0.5, 1.0, 5.0; Pe=0.1, 0.3, 0.5, 1.0, 5.0; Re=0.1, 0.3, 0.5, 1.0; α=5, 10, 15, 20, 25 to have the results below:

We formulated and solved the problem of the oscillatory flow of soil mineral salt water in a bifurcating green plant, as seen in sections 2. We assumed that the aspect ratio is less than or equal to one (i.e. $\Re \leq 1$) and that the flow depends on δ_1^2, M^2, N^2, Gr/Gc, Pe_m, Re and α. For these, Table 1 – Table 12 show the computed results for the concentration and velocity factors for varied values of δ_1^2, M^2, N^2, Gr/Gc, Pe_m, Re and α. The results show that the increase in the chemical reaction rate, Hartmann number (for $0.1 \leq M^2 \leq 1.0$), Heat generation parameter, Grashof number (for $0.1 \leq Gr \leq 1.0$), Peclet number and Reynolds number increase the concentration and velocity, and specifically, the increase in the bifurcation angle decreases the concentration but increases the velocity. Furthermore, it is seen that for Hartmann number $M^2 \geq 5.0$ the velocity drops. It is noteworthy that these results are the same for the temperature factor.

Table 1. Velocity-Chemical reaction rate in the mother channel

r	δ_1^2 **=0.1**	δ_1^2 **=0.3**	δ_1^2 **=0.5**	δ_1^2 **=1.0**	δ_1^2 **=5.0**
0.0	0.36328199I	0.3594169I	0.36832071I	0.40132766I	0.46458836I
.02	0.35870131I	0.3528408I	0.361289835I	0.393084463I	0.457147460I
0.4	0.34592389I	0.3340905I	0.341214725I	0.369431871I	0.435158733I
0.6	0.32774512I	0.3059649I	0.310984651I	0.333312377I	0.399019265I
0.8	0.30845480I	0.2726520I	0.27483158I	0.288569369I	0.347062797I
1.0	0.29312320I	0.2389110I	0.24029550I	0.241952252I	0.270810982I

The chemical reaction rate depends on the chemical reaction coefficient, chemical diffusivity of the fluid, and the concentration gradient existing between the interacting fluids. The diffusion of the chemical at higher level into the lower one calls for a reaction. The chemical reaction leads to the required depletion of the chemicals in the system. It may be exothermic or endothermic, implying that heat is given out or absorbed. The resultant effect is that the fluid particles are energized. The soil mineral salt water may contain some substances naturally present in the soil or due to soil pollution, which may spark-off a chemical reaction. In particular, the increase in the rate of chemical reaction increases the concentration of the fluid (see Table 1).

Table 2. Concentration-Hartmann number in the daughter channel

r	M^2=0.1	M^2=0.3	M^2=0.5	M^2=1.0	M^2=5.0
0.0	0.85233112I	0.926268267 I	1.10760517I	1.6805132 I	-25.6140530 I
0.2	0.822471299 I	0.9341923514I	1.11453195 I	1.67164802I	-25.7198738I
0.4	0.733085598 I	0.957924783I	1.13509737 I	1.64357088I	-26.1712791 I
0.6	0.585736032 I	0.996920274I	1.16714937 I	1.59190413 I	-27.3780473 I
0.8	0.386294882 I	1.048850732I	1.20207659 I	1.50957570 I	-30.0496389 I
1.0	0.149848233 I	1.107476354 I	1.21727164 I	1.38715548 I	-35.2349411 I

Table 3. Velocity-Hartmann number in the mother channel

r	M^2=0.1	M^2=0.3	M^2=0.5	M^2=1.0	M^2=5.0
0.0	0.26390149I	0.31144090I	0.38768449I	0.57367349I	-24.622213 I
0.2	0.25839926I	0.30519273I	0.38054619I	0.56685124I	-30.783593I
0.4	0.24231368I	0.28709883I	0.36031536 I	0.55061250I	-49.171068 I
0.6	0.21686967 I	0.25903279I	0.33034302I	0.53598775I	-89.031315 I
0.8	0.18395116I	0.22382237I	0.29550927I	0.53595580I	-197.56867 I
1.0	0.14575602I	0.18467585I	0.26101958 I	0.55758637 I	-507.65644I

The soil water absorbed into the plant may be saline or slightly acidic in nature; therefore, it is electrolytic and magnetically susceptible. The chemical content exists as ions or charges. The motion of these ions in the presence of the Earth magnetic field produces electric currents. In addition, the action of the magnetic field on the currents generates a mechanical force, the Lorentz force, which modifies the flow. The Lorentz force tends to fractionalize and polarize the fluid chemical contents such that they cluster around the magnetic field. Similarly, the freezing of the velocity makes the fluid to be concentrated in the region. This may accounts for what is seen in Table 2. Even so, the analysis shows that any increase in the Hartmann number in the range of $0.1 \leq M^2 \leq I.0$ tends to increase the velocity whereas it decreases for $M^2 \geq 5.0$ (see Table 3). In many flow problems, the Hartmann number is known to freeze up the velocity field. The re-ordering of the flow in the range of $0.1 \leq M^2 \leq I.0$ here could be due to the oscillatory effect.

Table 4. Velocity-Heat exchange parameter in the mother channel

r	N^2=0.1	N^2 =0.3	N^2 =0.5	N^2 =1.0	N^2 =5.0
0.0	0.36288567I	0.364138365I	0.366835387I	0.393909984I	0.45303201I
0.2	0.35604614I	0.357265425I	0.359881170I	0.385670013I	0.44867602I
0.4	0.33652489I	0.337648299I	0.340029822I	0.362015323I	0.42068217I
0.6	0.30716323I	0.308139264I	0.310157161I	0.325859782I	0.38075685I
0.8	0.27216121I	0.272948694I	0.274492647I	0.281025051I	0.32311451I
1.0	0.2361398I	0.23669126I	0.23762501 I	0.23800023 I	0.23861976 I

Furthermore, in heat-involving systems, heat is either generated or absorbed. In whichever way, the existence of the heat looses the fluid particles from the grip of viscosity and grants them buoyancy. The energization of the fluid particles tends to increase the velocity structures, as seen in Table 4.

Table 5. Concentration-Grashof number in the daughter channel

r	Gr =**0.1**	Gr =**0.3**	Gr =**0.5**	Gr =**1.0**
0.0	0.595079506I	0.856698596I	1.040541121	12.4683188 I
0.2	0.599892358I	0.861351285I	1.044262251	12.3971754 I
0.4	0.614340825 I	0.875306569I	1.055382521	12.1826592 I
0.6	0.638390290 I	0.898371555I	1.073311071	11.8206646 I
0.8	0.671768567 I	0.929609604I	1.095524311	11.3035244 I
1.0	0.713644151I	0.96641762 I	1.115257941	10.6182726I

Table 6. Velocity-Grashof number in the mother channel

r	Gr =**0.1**	Gr =**0.3**	Gr =**0.5**	Gr =**1.0**
0.0	0.071714445I	0.21835365I	0.365958131	0.73471924I
0.2	0.070395046I	0.21425584I	0.359031881	0.72071264I
0.4	0.066634591I	0.20256367I	0.339261291	0.68071681I
0.6	0.061003314I	0.18499366I	0.309514541	0.62047294I
0.8	0.054341729I	0.16407779I	0.274015421	0.54842278I
1.0	0.047464895I	0.14252222I	0.2373632 I	0.47391178 I

Similarly, the increase in the concentration/thermal gradient, which leads to an increase in the free convection or buoyancy force, may have resulted from the increase in the external/environmental temperature. The buoyancy force or Grashof number reduces the viscosity of the fluid and energizes its flow velocity. The results also show that the Grashof number in the range of $0.1 \leq Gc \leq I.0$ tends to increase the concentration and velocity (see Table 5 and 6). These results quite agree with [4,10,13].

Table 7. Concentration-Peclet number in the daughter channel

r	Pe =**0.01**	Pe =**0.05**	Pe =**0.1**	Pe =**0.5**	Pe =**1.0**
0.0	1.0405369 I	1.04054027I	1.0405445 I	1.0405785 I	1.0406211I
0.2	1.0442580 I	1.0442614 I	1.0442657 I	1.0442998 I	1.0443425 I
0.4	1.0553782 I	1.0553817 I	1.0553860 I	1.0554205 I	1.0554637 I
0.6	1.0733067I	1.0733102 I	1.0733146 I	1.0733497 I	1.0733937I
0.8	1.0955198I	1.0955234I	1.0955279 I	1.0955638 I	1.0956087 I
1.0	1.1152534 I	1.1152570 I	1.1152616 I	1.1152982 I	1.1153439 I

Table 8. Velocity-Peclet number in the daughter channel

r	Pe =**0.01**	Pe =**0.05**	Pe =**0.1**	Pe =**0.5**	Pe =**1.0**
0.0	92.876895 I	92.8772251 I	92.8776383 I	92.8809434I	92.8850749 I
0.2	93.065874I	93.0662053I	93.0666193 I	93.0699311 I	93.0740709 I
0.4	93.631215 I	93.6315646I	93.6319811 I	93.6353130 I	93.6394779 I
0.6	94.578946 I	94.5792828 I	94.5797035 I	94.5830690 I	94.5872760 I
0.8	95.949220 I	95.9495616 I	95.9499884 I	95.9534026 I	95.9576704 I
1.0	97.862164 I	97.8625123I	97.8629476I	97.8664298 I	97.8707825 I

Additionally, Peclet number depends on the size of the kinetic viscosity and diffusivities of the fluid. The analysis shows that the higher it is the better the flow (see Tables 7 and 8). Especially for the velocity, the results perfectly agree with [13]).

Table 9. Concentration-Reynolds number in the daughter channel

r	Re =**0.1**	Re =**0.3**	Re =**0.5**	Re =**1.0**	Re =**5.0**
0.0	0.34684704 I	1.04054112I	1.73423519 I	3.46847039 I	17.3423519 I
0.2	0.34808741 I	1.04426224 I	1.74043707 I	3.48087414 I	17.4043707 I
0.4	0.35179417I	1.05538252I	1.75997087I	3.51794174I	17.5897087I
0.6	0.35777035I	1.07331106I	1.78885177I	3.57770353I	17.8885177I
0.8	0.36517477I	1.09552430I	1.82587383I	3.65174766I	18.2587383I
1.0	0.37175264I	1.11535793I	1.85876321I	3.71752643I	18.5876322I

Table 10. Velocity-Reynolds number in the daughter channel

r	Re =**0.1**	Re =**0.3**	Re =**0.5**	Re =**1.0**
0.0	309.5910260I	928.77307801I	1547.955130I	3095.910260I
0.2	310.2209603I	930.66288090I	1551.104802I	3102.209603I
0.4	312.1054933I	936.31647990I	1560.527466I	3121.054933I
0.6	315.2645566I	945.79366980I	1576.322783I	3152.645566I
0.8	319.8321566I	959.49646980I	1599.160783I	3198.321566I
1.0	326.2086648I	978.62599440I	1631.043324I	3262.086648I

Moreover, the flow in the mother channel is laminar and Poiseuille. Therefore, its Reynolds number is moderate in the range of the flow. However, towards the nodal point/bifurcation or entry into the daughter channel, the Reynolds number, hence the momentum rises due to the change in the geometrical configuration. This increase positively affects the concentration and velocity structure (Tables 9 and 10). For the velocity, result is in good agreement with [4,13]).

Table 11. Concentration-bifurcation angles in the daughter channel

r	α =5	α =10	α =15	α =20	α =25
0.0	0.3003087I	-917.6626I	-1.71523 E+5I	-7.08514 E+6I	-1.2835 E+8I
0.2	0.2957192I	-927.0039I	-1.72158 E+5I	-7.10721 E+6I	-1.29816 E+8I
0.4	0.2819042I	-939.0122I	-1.74064 E+5I	-7.17342 E+6I	-1.29816 E+8I
0.6	0.2587052I	-965.6408I	-1.77239 E+5I	-7.28375 E+6I	-1.31648 E+8I
0.8	0.2257918I	-1002.812I	-1.81679 E+5I	-7.43815 E+6I	-1.34213 E+8I
1.0	0.1825630I	-1050.420I	-1.87381 E+5I	-7.63658 E+6I	-1.37509 E+8I

Table 12. Velocity-bifurcation angles in the daughter channel

r	α =**5**	α =**10**	α =**15**	α =**20**	α =**25**
0.0	6.191821I	5662.903014I	1.192474 E+6I	6.788532E+7I	1.81849 E+9I
0.2	6.204419I	5674.77439I	1.194889 E+6I	6.802169E+7I	1.82214E+9I
0.4	6.242110I	5710.20318I	1.202124 E+6I	6.843059E+7I	1.83307 E+9I
0.6	6.305291I	5768.85326I	1.2141593E+6I	6.911165E+7I	1.85128E+9I
0.8	6.524173I	5850.32830I	1.2309725 E+6 I	7.00644 E+7 I	1.87676 E+9 I
1.0	6.524173I	5954.19682 I	1.252536 E+6 I	7.12883E+7 I	1.90952 E+9 I

Similarly, Table 11 shows that the increase in the bifurcation angle decreases the quantity of soil mineral salt water being transported.

Furthermore, the increase in the bifurcation angle narrows down the diameter of the daughter channel. This tends to increase in the inlet pressure, which in turn increases the flow velocity. This may account for what is seen in Table 12. This result agrees with those of [2,4].

Usually, oscillatory characteristics produce several flow patterns such as turbulent zones, and vortices, which lead to loss of energy for the flow and destroy the axial velocity. These tend to weaken or delay the transport of materials. Therefore, the increase in the flow variables has some attendant implications on the growth and yield of the plant (crop). In particular, studies have revealed that the decrease in the velocity due to the magnetic field reduces the rate at which soil mineral salt water is transported from the soil via the roots, through the trunk and branches to the leaves. The variation in the saline or acidic levels of the soil, hence the magnetic field tends to explain why some crops do well in some regions than in others. The analyses of this model show that the same magnetic field (in the range of $0.1 \leq M^2 \leq 1.0$), which reduces the velocity in a normal/non-oscillatory flow enhances the transport velocity in the oscillating situation. Since both non-oscillating and oscillating flows take place at the same time in the green plant, it suffices to say that the effect of magnetic field on the velocity structure in the oscillatory flow tends to cushion the adverse effects of magnetic field in the non-oscillatory flow. Two, the increase in the concentration of the fluid in the plant increases the inflow of the soil mineral water, which is usually at lower osmotic pressure into the plant. The continual inflow and exhaustion of the soil mineral salt water in the plant helps in making nutrients available to it, and this in turn enhances its growth and yield.

4 Conclusion

This study presents an analytic model of the oscillatory flow of soil mineral salt water in a bifurcating green plant. The study is focused on the effects of the chemical reaction rate, nature of the soil (magnetic susceptibility), heat generation/absorption parameter, Grashof number, Peclet number, and Reynolds number and bifurcation angles on the concentration and velocity factors. The results show that the increase in the chemical reaction rate, Hartmann number (for $0.1 \leq M^2 \leq 1.0$), Heat generation parameter, Grashof number for $0.1 \leq Gr \leq 1.0$), Peclet number, Reynnolds number increase the concentration and velocity, and specifically, the increase in the bifurcation angle decreases the concentration but increases the velocity. Furthermore, it is seen that for Hartmann number $M^2 \geq 5.0$ the velocity drops. The increase in the flow variables has some resultant implications on the growth and yield of the plant. In particular, since the normal/non-oscillatory and oscillatory flows take place at the same time in the plant, the increase in the velocity due to the increase in the magnetic field in the range of $0.1 \leq M^2 \leq 1.0$ in the oscillatory flow tends to cushion the adverse effects of magnetic field in the non-oscillatory flow. Furthermore, the increase in the concentration of the fluid in the plant enhances the inflow of the soil mineral salt into it, and this in turn enhances its growth and yield.

Competing Interests

Authors have declared that no competing interests exist.

References

[1] Bestman AR. Global models for the biomechanics of green plants, part 1. International Journal of Energy Research. 1991;16:677-684.

[2] Smith FT, Jones MA. Modeling of multi–branching tube flows: Large flow rates and dual solutions. IMA Journal of Mathematical Medical Biology. 2003;20:183–204.

[3] Tadjar M, Smith FT. direct simulation and modeling of basic 3-dimensional bifurcating tube flow. Journal of Fluid Mechanics. 2004;519:1-32.

[4] Okuyade WIA, Abbey TM. Analytic study of blood flow in bifurcating arteries, part 1-effects of bifurcation angle and magnetic field. International Organization of Scientific Research Journal of Mathematics. 2015;I.D:G54040 - (In press).

[5] Asadolah Malekzadeh, Amir Heydarinasab, Bahram Dabir. Magnetic field effect on fluid flow characteristic in a pipe for laminar flow. Journal of Mechanical Science and Technology. 2011; 25:333-339.

[6] Venkateswalu S, Suryanarayama Rao KV, Rambupal Reddy B. Finite difference analysis on convective heat transfer flow through porous medium in vertical channel with magnetic field. Indian Journal Applied Mathematics and Mechanics. 2011;7(7):74-94.

[7] Paresh Vyas Srivastava N. Oscillatory flow in a vertical channel filled with porous medium with radiation and dissipation effects. Walailak Journal of Science and Technology. 2013;10(5):

[8] Asghar AA. Analytic solution of oscillatory flow in channel for Jeffery fluid. Journal of Aerospace Engineering. 2014;27:644-651.

[9] Das S, Jana RN, Makinde OD. Mixed convection magneto-hydrodynamic flow in a channel filled with Nano-fluids. Elsevier Journal of Engineering Science and Technology. 2015;244-255.
DOI: http://dx.doi.org/10.1016/j.jestch 2014.12009

[10] Sharma PR, Kalpna Sharma, Tripti Mehta. Radiative and free convective effects on MHD flow through a porous medium with periodic wall temperature and heat generation or absorption. International Journal of Mathematical Archive. 2014;5(9):119-128.

[11] Okuyade WIA. MHD blood flow in bifurcating porous fine capillaries. African Journal of Science Research. 2015;4(4):56-59.

[12] Mathew A, Singh KD. Span-wise fluctuating MHD convective heat and mass transfer flow through a porous medium in a vertical channel with thermal radiation and chemical reaction. International Journal of Heat and Technology. 2015;33(2).
DOI: 10.1820/Ijht.330222

[13] Krishna MV, Basha SC. MHD free convection three dimensional flow through a porous medium between two vertical plates. IOSR Journal of Mathematics. 2016;88-105.
DOI: 10.9790/5728-121288105

[14] Ahmed R, Jewel BM, Uddin R, Islam MM, Ahmed S. Chemical reaction and radiative MHD heat and mass transfer flow with temperature dependent viscosity past an isothermal oscillating cylinder. Physical Science International Journal. 2016;12(1):1-9.

Appendices

$$D_1 = \frac{1}{I_o\left(\lambda_8^{1/2}\right)}\left[\Phi_w - \frac{I_o\left(\lambda_8^{1/2} r\right)}{2}\lambda_8^{1/2} C_1 \frac{I_1\left(\lambda_6^{1/2}\right)}{\lambda_6^{1/2}}\right]$$

$$C_1 = \frac{1}{I_o\left(\lambda_6^{1/2}\right)}\left[\Phi_w - \frac{I_o\left(\lambda_6^{1/2}\right)}{2}\lambda_6^{1/2} B_1 \frac{J_1\left(\lambda_4^{1/2}\right)}{\lambda_4^{1/2}}\right]$$

$$B_1 = \frac{1}{J_o\left(\lambda_4^{1/2}\right)}\left[\Phi_w - J_o\left(\lambda_4^{1/2}\right)\lambda_4^{1/2} A_1 \frac{J_1\left(\lambda_2^{1/2}\right)}{\lambda_2^{1/2}}\right]$$

$$A_1 = \frac{1}{J_o\left(\lambda_2^{1/2}\right)}\left[\Phi_w - J_o\left(\lambda_2^{1/2}\right)\frac{\pi\lambda_2^{1/2}}{2}\gamma\Re\varepsilon Pe_h \aleph\right]$$

$$V_1 = -\frac{1}{I_o(M_1)}\left\{-M_1 I_o(M_1)\left[-\frac{\Re\aleph}{2} + GrD_1\frac{I_1(\lambda_8^{1/2})}{\lambda_6^{1/2}} + -\frac{1}{20} - \frac{\lambda_6}{114} + M_1^2\left(\frac{1}{16} + \frac{\lambda_6}{192}\right)\right]\right.$$
$$\left. + \left(-\frac{M_1}{2} + \frac{M_1^2}{4}\right)\left[\frac{\Re\aleph I_1(M_1)}{M_1} - 2GrD_1\left(\frac{I_1(\lambda_8^{1/2})}{\lambda_8^{1/2}}\ \frac{M_1^2}{6} - \frac{M_1^2\lambda_8}{40}\right) + \frac{1}{6} + \frac{\lambda_6}{80} + M_1^2\left(\frac{r^4}{16} + \frac{\lambda_6 r^6}{192}\right)\right]\right\}$$

$$K_1 = \frac{1}{I_o\left(\lambda_{16}^{1/2}\Re\alpha x\right)}\left[\gamma_2\Phi_w - \frac{I_o\left(\lambda_{16}^{1/2}\Re\alpha x\right)}{2}\lambda_{16}^{1/2} G_1 \Re\alpha x \frac{I_o\left(\lambda_{14}^{1/2}\Re\alpha x\right)}{\lambda_{14}^{1/2}}\right]$$

$$G_1 = \frac{1}{I_o\left(\lambda_{14}^{1/2}\Re\alpha x\right)}\left[\gamma_2\Phi_w - \frac{I_o\left(\lambda_{14}^{1/2}\Re\alpha x\right)}{2}\lambda_{14}^{1/2} F_1 \Re\alpha x \frac{J_1\left(\lambda_{12}^{1/2}\Re\alpha x\right)}{\lambda_{12}^{1/2}}\right]$$

$$F_1 = \frac{1}{J_o\left(\lambda_{12}^{1/2}\Re\alpha x\right)}\left[\gamma_2\Phi_w - \frac{J_o\left(\lambda_{12}^{1/2}\Re\alpha x\right)}{2}\pi\lambda_{12}^{1/2} E_1 \Re\alpha x \frac{J_1\left(\lambda_{10}^{1/2}\Re\alpha x\right)}{\lambda_{10}^{1/2}}\right]$$

$$E_1 = \frac{1}{J_o\left(\lambda_{10}^{1/2}\Re\alpha x\right)}\left[\gamma_2\Phi_w - \frac{J_o\left(\lambda_{10}^{1/2}\Re\alpha x\right)}{2}\pi\lambda_{10}^{1/2}\left[-\gamma^2\Re^2\varepsilon^2 Pe_h\left(\aleph + \aleph_1 x\right)\frac{\left(\Re\alpha x\right)^2}{2}\right.\right.$$
$$\left.\left. + 2\gamma^2\Re^2\varepsilon^2 D_1 \Re\alpha x \frac{I_1\left(\lambda_6^{1/2}\Re\alpha x\right)}{\lambda_6^{1/2}}\right]\right]$$

$$V_2 = -\frac{1}{I_o(M_1\Re\alpha x)}\left\{-M_1\Re\alpha x I_o(M_1\Re\alpha x)\left\{-\frac{\Re\aleph_1 x(\Re\alpha x)}{2} + Gc\left[\frac{K_1 I_1(\lambda_{16}^{1/2}\Re\alpha x)}{\lambda_{16}^{1/2}} + \lambda_{16}^{1/2}G_1\left(\frac{(\Re\alpha x)I_1(\lambda_{16}^{1/2}\Re\alpha x)}{\lambda_{16}^{1/2}} + \frac{\lambda_{14}(\Re\alpha x)^4}{64} + \frac{\lambda_{14}\lambda_{16}(\Re\alpha x)^6}{384}\right)\right] + \frac{M_1^2}{4}\left[\frac{\Re\aleph_1(\Re\alpha x)^3}{3} - 2Gc\left[K_1\left(\frac{(\Re\alpha x)^3}{3} + \frac{\lambda_{16}(\Re\alpha x)^5}{20}\right) + \lambda_{16}^{1/2}G_1\left(\frac{(\Re\alpha x)I_1(\lambda_{16}^{1/2}\Re\alpha x)}{2\lambda_{16}^{1/2}} + \frac{\lambda_{14}(\Re\alpha x)^4}{64} + \frac{\lambda_{14}\lambda_{16}(\Re\alpha x)^6}{384}\right)\right]\right]\right\} + \left(-\frac{M_1\Re\alpha x}{3} + \frac{M_1^3(\Re\alpha x)^3}{4}\right)\left\{-\frac{\Re\aleph_1 x I_1(M_1\Re\alpha x)}{M_1} - 2Gc\left[K_1\left(\frac{I_1(M_1\Re\alpha x)}{M_1} + \frac{\lambda_{16}(\Re\alpha x)^4}{16} + \frac{M_1^2\lambda_{16}(\Re\alpha x)^5}{80}\right) + \lambda_{16}^{1/2}G_1\left(\frac{(\Re\alpha x)I_1(M_1\Re\alpha x)}{2M_1} + \frac{\lambda_{14}(\Re\alpha x)^4}{64} + \frac{\lambda_{14}M_1(\Re\alpha x)^6}{384}\right) + \frac{\lambda_{16}(\Re\alpha x)^4}{32} + \frac{\lambda_{16}M_1^2(\Re\alpha x)^6}{192} + \frac{\lambda_{14}\lambda_{16}(\Re\alpha x)^6}{384} + \frac{\lambda_{14}\lambda_{16}M_1^2(\Re\alpha x)^8}{2048}\right]\right\}\right\}$$

$$\lambda_2 = \sqrt{\left\{\frac{1}{2}\left(-\left(-M_1^2 + 2N^2M_1^2 + 2M_1^2 - N^2\delta_1^2 - M_1^4 - 2\gamma\Re\varepsilon\right) + \sqrt{\left(\left(-M_1^2 + 2N^2M_1^2 + 2M_1^2 - N^2\delta_1^2 - M_1^4 - 2\gamma\Re\varepsilon\right)^2 + 4\left(-M_1^2\delta_1^2\gamma\Re\varepsilon + \gamma^2\Re^2\varepsilon^2\right)\right)}\right\}}$$

$$\lambda_4 = \sqrt{\left\{\frac{1}{2}\left(-\left(-M_1^2 + 2N^2M_1^2 + 2M_1^2 - N^2\delta_1^2 - M_1^4 - 2\gamma\Re\varepsilon\right) - \sqrt{\left(\left(-M_1^2 + 2N^2M_1^2 + 2M_1^2 - N^2\delta_1^2 - M_1^4 - 2\gamma\Re\varepsilon\right)^2 + 4\left(-M_1^2\delta_1^2\gamma\Re\varepsilon + \gamma^2\Re^2\varepsilon^2\right)\right)}\right\}}$$

$$\lambda_6 = i\sqrt{\left\{\frac{1}{2}\left(-\left(-M_1^2 + 2N^2M_1^2 + 2M_1^2 - N^2\delta_1^2 - M_1^4 - 2\gamma\Re\varepsilon\right) + \sqrt{\left(\left(-M_1^2 + 2N^2M_1^2 + 2M_1^2 - N^2\delta_1^2 - M_1^4 - 2\gamma\Re\varepsilon\right)^2 + 4\left(-M_1^2\delta_1^2\gamma\Re\varepsilon + \gamma^2\Re^2\varepsilon^2\right)\right)}\right\}}$$

$$\lambda_8 = i\sqrt{\left\{\frac{1}{2}\left(-\left(-M_1^2 + 2N^2M_1^2 + 2M_1^2 - N^2\delta_1^2 - M_1^4 - 2\gamma\Re\varepsilon\right) - \sqrt{\left(\left(-M_1^2 + 2N^2M_1^2 + 2M_1^2 - N^2\delta_1^2 - M_1^4 - 2\gamma\Re\varepsilon\right)^2 + 4\left(-M_1^2\delta_1^2\gamma\Re\varepsilon + \gamma^2\Re^2\varepsilon^2\right)\right)}\right\}}$$

$$\lambda_{10} = \sqrt{\frac{1}{2}\left\{-\left(-\delta_1^2M_1^2 - \left(N^2 - M^2\right)\left(\delta_1^2 - M^2\right) - M_1^2N^2\right) + \sqrt{\left(\left(-\delta_1^2M_1^2 - \left(N^2 - M^2\right)\left(\delta_1^2 - M^2\right) - M_1^2N^2\right)^2 - 4\left(\gamma\Re\varepsilon\left(M_1^2N^2\delta_1^2 - M_1^2N^2 - M_1^2\delta_1^2\right)\right)\right)}\right\}}$$

$$\lambda_{12} = \sqrt{\frac{1}{2}\{-\left(-\delta_1^2 M_1^2 - \left(N^2 - M^2\right)\left(\delta_1^2 - M^2\right) - M_1^2 N^2\right) - \sqrt{\left(\left(-\delta_1^2 M_1^2 - \left(N^2 - M^2\right)\left(\delta_1^2 - M^2\right) - M_1^2 N^2\right)^2 - 4\left(\gamma\Re\varepsilon\left(M_1^2 N^2 \delta_1^2 - M_1^2 N^2 - M_1^2 \delta_1^2\right)\right)\right)}\}}$$

$$\lambda_{14} = i\sqrt{\sqrt{\frac{1}{2}\{-\left(-\delta_1^2 M_1^2 - \left(N^2 - M^2\right)\left(\delta_1^2 - M^2\right) - M_1^2 N^2\right) + \sqrt{\left(\left(-\delta_1^2 M_1^2 - \left(N^2 - M^2\right)\left(\delta_1^2 - M^2\right) - M_1^2 N^2\right)^2 - 4\left(\gamma\Re\varepsilon\left(M_1^2 N^2 \delta_1^2 - M_1^2 N^2 - M_1^2 \delta_1^2\right)\right)\right)}\}}}$$

$$\lambda_{16} = i\sqrt{\sqrt{\frac{1}{2}\{-\left(-\delta_1^2 M_1^2 - \left(N^2 - M^2\right)\left(\delta_1^2 - M^2\right) - M_1^2 N^2\right) - \sqrt{\left(\left(-\delta_1^2 M_1^2 - \left(N^2 - M^2\right)\left(\delta_1^2 - M^2\right) - M_1^2 N^2\right)^2 - 4\left(\gamma\Re\varepsilon\left(M_1^2 N^2 \delta_1^2 - M_1^2 N^2 - M_1^2 \delta_1^2\right)\right)\right)}\}}}$$

Peer-review history:
The peer review history for this paper can be accessed here (Please copy paste the total link in your browser address bar)
http://sciencedomain.org/review-history/17836